

BALANCE CONTROL OF ARTICULATED ROVERS WITH ACTIVE SUSPENSION

Gregory McDermott, Mahmoud Tarokh and Lorena Mireles

*Department of Computer Science
San Diego State University
San Diego, CA 92182-7720, U.S.A.*

Abstract: The paper proposes a simple and computationally efficient method for the modelling of highly articulated rovers traversing rough terrain. The method is based on the propagation of position and orientation velocities through wheels and various joints and linkages of the rover. These velocity equations are combined to form the Jacobian matrix of the rover that relates the position and orientation of the rover to various active (actuated) and passive rover joint variables. A rearrangement of the Jacobian equation allows determining the actuation variables for motion control. Rover balance control for avoiding tipover is achieved by actuating the suspension joints. This is done through a pseudo-inverse method which optimizes a balance performance criterion. To illustrate the kinematics modelling and balance control concepts, the method is applied to a rover similar to the NASA's Sample Return Rover.

Keywords: Rover control, Rover Kinematics, Articulated Rovers.

1. INTRODUCTION

Articulated rovers will be used increasing in diverse applications such as terrestrial and planetary explorations (Schenker et al 2003), (Volpe 2003), forestry (Gonthier 1998), agriculture (Baerveldt 2002) mining industries (Cunningham et al 1998), defense applications and hazardous material handling and de-mining (DeBolt et al 1997). Rovers with active suspension mechanisms are capable of modifying their configurations by adjusting their suspension linkages and joints so as to change their center of mass, thus avoiding tipover while traversing rough and sloppy terrain.

Rovers with adjustable suspension system have been considered by Sreenivasan and Waldron (1996) for a specific vehicle. More recently, Iagnemma and Dubowsky (2003) presented stability-based suspension control for a specific rover using an essentially geometric approach and performing a rather complex optimization procedure.

In a previous paper (Tarokh and McDermott 2005), we developed full kinematics models of articulated rovers and provided analysis of these rovers. The purpose of the present paper is twofold. First, is to present an alternative method for kinematics modeling of articulated rovers, which is straightforward, appealing, and computationally efficient. Second is to develop an optimization technique and incorporate it within the kinematics formulation to achieve simultaneous motion and balance control for rovers with active suspension mechanisms. The developed methodology is applied to a rover for demonstration purposes.

2. KINEMATICS MODEL DEVELOPMENT

We define an articulated rover with active suspension system (ARAS) as a wheeled mobile robot consisting of a main body connected to wheels via a set of linkages and joints that can be adjusted, some actively and some passively for keeping the rover balanced. The active linkages and joints have actuators through which their values can be controlled, whereas passive ones change their values to comply with the terrain topology.

The goal of balance control is to determine the actuation quantities for balancing the rover to avoid tipover. In order to achieve this, we must determine the contributions of each wheel and suspension mechanism to the overall motion of the rover. We attach a number of frames starting from the wheel-terrain contact frame then going through the steering and suspension frames and finally to the rover reference frame. Since we are interested in the motion, we relate the translational and rotational velocities of the next frame in terms of the previous frame. Let $u_a = [x_a \ y_a \ z_a]^T$ and $u_b = [x_b \ y_b \ z_b]^T$ denote the position of the current and next frames, respectively. Similarly, let $\varphi_a = [\alpha_a \ \beta_a \ \gamma_a]^T$ and $\varphi_b = [\alpha_b \ \beta_b \ \gamma_b]^T$ be the orientation of the current and next frames, respectively, where α, β and γ are the rotation around x, y and z axis, or pitch, yaw and roll, respectively. The 3×1 translation velocity vector of the next frame b is dependent on the translational and

rotational velocities of the current frame a plus any translational velocity added to the frame b itself. This can be written as (Craig 2005)

$$\dot{u}_b = R_{b,a}(\dot{u}_a + \dot{\phi}_a \times p_b) + \dot{u}_{ob} \quad (1)$$

where $R_{b,a}$ and p_b are, respectively, the rotation matrix and position vector of the frame b relative to the frame a , and \dot{u}_{ob} is the translational velocity added to the frame b . The latter is zero if the joint associated with the frame b is not prismatic. The rotational velocity of the next frame b is dependent on the rotational velocity of the frame a plus any rotational velocity $\dot{\phi}_{ob}$ added to the frame b itself, i.e. (Craig 2005)

$$\dot{\phi}_b = R_{b,a} \dot{\phi}_a + \dot{\phi}_{ob} \quad (2)$$

We start at each wheel i ($i = 1, 2, \dots, n$) contact frame which has the translational and rotational velocities $\dot{u}_i = [\dot{x}_i \ \dot{y}_i \ \dot{z}_i]^T$ and $\dot{\phi}_i = [\dot{\alpha}_i \ \dot{\beta}_i \ \dot{\gamma}_i]^T$, and perform the frame to frame velocity propagation until we reach to the rover reference frame to obtain rover velocities $\dot{u}_r = [\dot{x}_r \ \dot{y}_r \ \dot{z}_r]^T$ and $\dot{\phi}_r = [\dot{\alpha}_r \ \dot{\beta}_r \ \dot{\gamma}_r]^T$. Let the joint variable vector that includes each wheel-terrain contact angle, steering angle, and various prismatic and revolute joint variables be denoted by the $v_i \times 1$ vector η_i . Then we will obtain an equation of the general form

$$\begin{pmatrix} \dot{u}_r \\ \dot{\phi}_r \end{pmatrix} = J_i \begin{pmatrix} \dot{u}_i \\ \dot{\phi}_i \\ \dot{\eta}_i \end{pmatrix}; \quad i = 1, 2, \dots, n \quad (3)$$

where J_i is the Jacobian matrix of the wheel i . Note that the wheel translational and rotational velocity vectors \dot{u}_i and $\dot{\phi}_i$ include various slips. For example $\dot{x}_i = r_i \dot{\theta}_i + \dot{\zeta}_{roll-i}$ where r_i is the radius of wheel i , $\dot{\theta}_i$ is the angular velocity of that wheel, and $\dot{\zeta}_{roll-i}$ is the rolling slip rate. Similarly \dot{y}_i and \dot{z}_i can, respectively, have side slip $\dot{\zeta}_{side-i}$ and bounce $\dot{\zeta}_{bnce-i}$ (up and down off the terrain movement) components. In addition, $\dot{\alpha}_i$, $\dot{\beta}_i$ and $\dot{\gamma}_i$ can be associated, respectively, with tilt $\dot{\zeta}_{tilt-i}$, sway $\dot{\zeta}_{sway-i}$ and turn $\dot{\zeta}_{turn-i}$ slip rate components. In practice some of these slip components are unnecessary due to terrain topology and surface conditions, the path to be traversed (e.g. straight, serpentine, wavy) and mechanical arrangement of the wheels and suspension system.

Equation (3) describes the contribution of individual wheel motion and the connecting joints to the rover body motion. The net body motion is the composite effect of all wheels and can be obtained by combining (3) into a single matrix equation as

$$\begin{pmatrix} I_6 \\ \vdots \\ I_6 \end{pmatrix} \begin{pmatrix} \dot{u}_r \\ \dot{\phi}_r \end{pmatrix} = J \begin{pmatrix} \dot{u}_w \\ \dot{\phi}_w \\ \dot{\eta} \end{pmatrix} \quad (4)$$

where the composite identity matrix on the left is $6n \times n$, $\dot{u}_w = (\dot{u}_1 \ \dot{u}_2 \ \dots \ \dot{u}_n)^T$ and $\dot{\phi}_w = (\dot{\phi}_1 \ \dot{\phi}_2 \ \dots \ \dot{\phi}_n)^T$

are $3n \times 1$ vectors of composite wheel velocities, and $\dot{\eta}$ is the $v \times 1$ vector of the joint variables which has both active (actuated) and passive joints. Note that in general some wheels share common suspension links and joints so that $v \leq \sum_{i=1}^n v_i$. The composite Jacobian matrix of the rover J has a dimension of $6n \times (6n + v)$.

2.1 Example

The articulated rover with active suspension (ARAS) to be considered here is similar to the JPL Sample Return Rover shown in Fig.1. The schematic diagram of ARAS to be analyzed is shown in Fig. 2. The rover has four wheels with each independently actuated and rotation angles subscripted with a clockwise direction so that θ_1, θ_4 are for the left side and θ_2, θ_3 are for the right side. At either side of the rover, two legs are connected via an adjustable hip joint. In Fig. 2 the hip angles on the left and right sides are denoted as $2\sigma_1$ and $2\sigma_2$, respectively. These joints are actuated and used for balancing the rover. The two hips are connected to the body via a differential which has an angle ρ on the left side and $-\rho$ on the right side. On a flat surface ρ is zero but becomes non-zero when one side moves up or down with respect to the other side. The differential joint ρ is passive (unactuated) and provides for the compliance with the terrain. The wheels are steerable with steering angles denoted by ψ_i . The wheel terrain contact angle δ_i is the angle between the z-axes of the i -th wheel axle frame A_i and contact coordinate frame C_i as shown in Fig. 3.

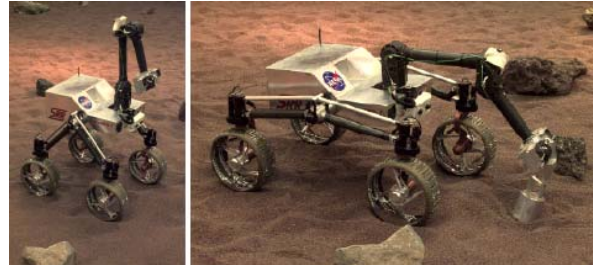


Fig. 1 The JPL's sample return rover

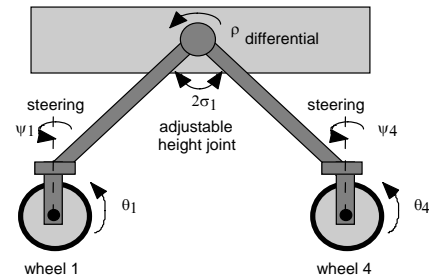


Fig. 2 Schematic diagram of the left side of ARAS

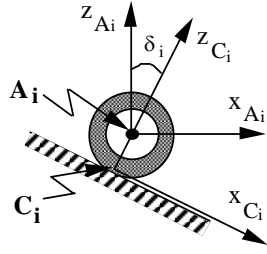


Fig. 3 Definition of contact angle

In order to derive the kinematics equations, we must assign coordinates frames. Fig. 4 illustrates our choice of coordinate frames for the left side of the rover. The right side is assigned similar frames. In Fig. 4, R is the rover reference frame whose origin is located on the center of gravity of the rover, its x-axis along the rover straight line forward motion, its y-axis across the rover body and its z-axis represents the up and down motion. The differential frame D has a vertical (along z-axis) offset denoted by k_1 and a horizontal distance of k_2 from D. The distance from the differential to the hip, denoted by k_3 , is half the width of the rover. We now introduce three more frames, all of which have origin at the wheel axle. The length of the legs from the hip to the wheel axle is k_4 . The hip frames H_1, \dots, H_4 for the four wheels are obtained from the differential frame by rotation and translation as shown with the Denavit-Hartenberg (D-H) parameters $\gamma_{dh}, d_{dh}, a_{dh}$ and α_{dh} in Table 1 and in Fig 3. Similarly the steering frames S_1, \dots, S_4 and axle frames A_1, \dots, A_4 are defined in Table 1 and Fig 3.

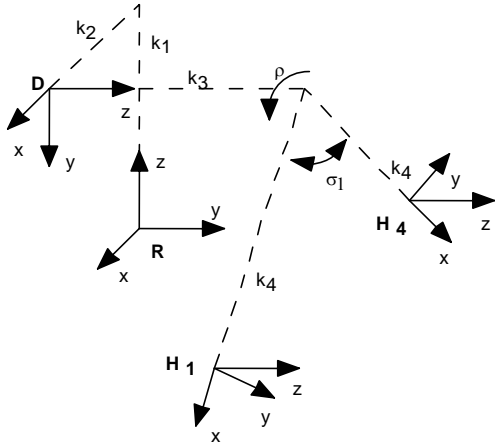


Fig. 4 Reference R, differential D, and hip H coordinate frames

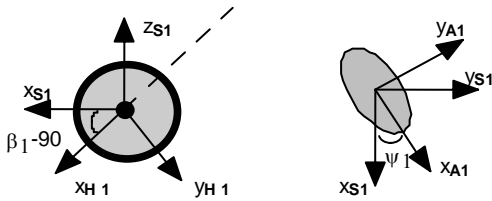


Fig. 5 Side (left figure) and top views of wheel 1

Frame	γ_{dh}	d_{dh}	a_{dh}	α_{dh}
D	0	k_1	k_2	-90
H1	$90 - \sigma_1 + \rho$	k_3	k_4	0
H2	$90 - \sigma_2 - \rho$	$-k_3$	k_4	0
H3	$90 + \sigma_3 - \rho$	$-k_3$	k_4	0
H4	$90 + \sigma_4 + \rho$	k_3	k_4	0
S1	$\sigma_1 - 90$	0	0	90
S2	$\sigma_2 - 90$	0	0	90
S3	$\sigma_3 - 90$	0	0	90
S4	$\sigma_4 - 90$	0	0	90
A1	ψ_1	0	0	0
A2	ψ_2	0	0	0
A3	ψ_3	0	0	0
A4	ψ_4	0	0	0

Table 1 D-H Parameters for the ARAS

We must now use the basic frame to frame equations (1)-(2) and go through the frames sequentially from wheel i terrain contact C_i , wheel axle A_i , steering S_i , hip H_i , differential D, and finally to the rover reference R. Equation (1)-(2) for the contact to the axle becomes

$$\begin{aligned} \dot{u}_{A_i} &= R_{A_i, C_i} \left(\dot{u}_{C_i} + \dot{\phi}_{C_i} \times \begin{pmatrix} 0 & 0 & r \end{pmatrix}^T \right) \\ \dot{\phi}_{A_i} &= R_{A_i, C_i} \dot{\phi}_{C_i} + \begin{pmatrix} 0 & -\dot{\delta}_i & 0 \end{pmatrix}^T \end{aligned} \quad (5)$$

where the rotation matrix is $R_{A_i, C_i} = \begin{pmatrix} c\delta_i & 0 & s\delta_i \\ 0 & 1 & 0 \\ -s\delta_i & 0 & c\delta_i \end{pmatrix}$, as

evident from Fig. 3. Note that wheel velocities at the terrain contact are denoted in (3) as $\dot{u}_{C_i} \equiv \dot{u}_i$ and $\dot{\phi}_{C_i} \equiv \dot{\phi}_i$. Next we form wheel i axle to steering velocity propagation as

$$\begin{aligned} \dot{u}_{S_i} &= R_{S_i, A_i} \left(\dot{u}_{A_i} + \dot{\phi}_{A_i} \times \begin{pmatrix} 0 & 0 & 0 \end{pmatrix}^T \right) \\ \dot{\phi}_{S_i} &= R_{S_i, A_i} \dot{\phi}_{A_i} + \begin{pmatrix} 0 & 0 & -\dot{\psi}_i \end{pmatrix}^T \end{aligned} \quad (6)$$

where $R_{S_i, A_i} = \begin{pmatrix} c\psi_i & -s\psi_i & 0 \\ s\psi_i & c\psi_i & 0 \\ 0 & 0 & 1 \end{pmatrix}$. The next in the chain

is the hip frame, and we can write

$$\begin{aligned} \dot{u}_{H_i} &= R_{H_i, S_i} \left(\dot{u}_{S_i} + \dot{\phi}_{S_i} \times \begin{pmatrix} 0 & 0 & 0 \end{pmatrix}^T \right) \\ \dot{\phi}_{H_i} &= R_{H_i, S_i} \dot{\phi}_{S_i} + \begin{pmatrix} 0 & 0 & -h_i \dot{\sigma}_i \end{pmatrix}^T \end{aligned} \quad (7)$$

with $R_{H_i, S_i} = \begin{pmatrix} s(h_i \sigma_i) & 0 & -c(h_i \sigma_i) \\ -c(h_i \sigma_i) & 0 & s(h_i \sigma_i) \\ 0 & 1 & 0 \end{pmatrix}$, $\sigma_4 = \sigma_1$,

$\sigma_3 = \sigma_2$, and $h_i = \begin{cases} 1 & i=1,2 \\ -1 & i=3,4 \end{cases}$. The differential frame

velocities are obtained from (1)-(2) and Table 1 as

$$\begin{aligned} \dot{u}_{D_i} &= R_{D_i, H_i} \left(\dot{u}_{H_i} + \dot{\phi}_{H_i} \times \begin{pmatrix} -k_4 & 0 & b_i k_3 \end{pmatrix}^T \right) \\ \dot{\phi}_{D_i} &= R_{D_i, H_i} \dot{\phi}_{H_i} + \begin{pmatrix} 0 & 0 & h_i \dot{\sigma}_i + b_i \dot{\rho}_i \end{pmatrix}^T \end{aligned} \quad (8)$$

$$\text{where } R_{D_i, H_i} = \begin{pmatrix} s(h_i \sigma_i + b_i \rho_i) & -c(h_i \sigma_i + b_i \rho_i) & 0 \\ c(h_i \sigma_i + b_i \rho_i) & s(h_i \sigma_i + b_i \rho_i) & 0 \\ 0 & 0 & 1 \end{pmatrix},$$

$$\rho_4 = \rho_1 = \rho, \rho_2 = \rho_3 = -\rho, \text{ and } b_i = \begin{cases} -1 & i=1,4 \\ 1 & i=2,3 \end{cases}.$$

Finally, the rover velocities are obtained as

$$\begin{aligned} \dot{u}_r &= R_{r, D_i} (\dot{u}_{D_i} + \dot{\phi}_{D_i} \times (-k_2 \quad -k_1 \quad 0)^T) \\ \dot{\phi}_r &= R_{r, D_i} \dot{\phi}_{D_i} + (0 \quad 0 \quad 0)^T \end{aligned} \quad (9)$$

Substituting recursively (5) through (8) into (9) we obtain an equation of the form (3) where $\dot{\eta}_i = (\dot{\rho}_i \quad \dot{\sigma}_i \quad \dot{\psi}_i \quad \dot{\delta}_i)^T$. Due to space limitation, the Jacobian matrices J_i and their elements are not given here but can be found in our technical report (Mireles, et al 2005). The elements of J_i are trigonometric functions of the joint variables ρ_i, σ_i, ψ_i and δ_i .

3. BALANCE CRITERION AND CONTROL

An active suspension system is used to operate the rover to achieve balanced rover configurations such that when the rover traverses on a slope or rough terrain, tipover is prevented. We must now define and quantify more precisely the notion of a balanced configuration and express it in terms of rover orientation angles and adjustable joint angles. To this end, we use wheel-terrain contact position vectors u_i , which represent vectors drawn from the rover reference point to the wheel-terrain contact point. Each consecutive pair of these vectors (i.e., u_i and u_{i+1}) form a plane denoted by π_i . The unit vector perpendicular to this plane is given by

$$\bar{s}_i = \frac{u_i \times u_{i+1}}{\|u_i \times u_{i+1}\|}; \quad i=1, \dots, n; \quad u_{n+1} = u_1 \quad (11)$$

Assuming that the rover reference frame R is at the center of rover mass, the rover unit gravity vector \bar{g} can be expressed in terms of pitch and roll angles as

$$\bar{g} = (s\phi_y \quad -s\phi_x c\phi_y \quad -c\phi_x c\phi_y)^T \quad (12)$$

Now we define the balance measure as the dot product between unit vectors \bar{s}_i and \bar{g} , i.e.

$$\mu_i = \bar{g}^T \bar{s}_i \quad (13)$$

Higher value of μ_i represents a more balanced rover. When the gravity vector \bar{g} lies in any of the planes π_i , the vectors \bar{g} and \bar{s}_i become orthogonal, resulting in $\mu_i = 0$. Tipover occurs when $\mu_i < 0$. We must now define an objective function whose optimization results in a balanced configuration. Consider minimization of an objective function of the form

$$f = a_1 \|\eta_a - \hat{\eta}_a\| + a_2 \beta_r^2 - a_3 \prod_{i=1}^n \mu_i \quad (14)$$

where η_a is the vector of actuated suspension joints and $\hat{\eta}_a$ is the nominal or desired values under normal

operating conditions (e.g., flat surface). The second term represents the rover roll which must be minimized to keep the rover body level. The product term is the tipover measures which must be maximized, hence the negative sign. Note that without the first term, minimizing f would result in a rover configuration that is maximally flat or spread out even when the rover moves over a flat surface. The weighting factors a_1, a_2 and a_3 place relative emphasis between achieving rover balancing and the desire to operate near the nominal configuration.

The balance and motion control problem may be stated as follows. Given the desired rover forward speed \dot{x}_d and heading γ_d , determine the commands to the wheel, and actuated joints, which include the steering, such that the rover maintains the desired forward speed and heading while minimizing the balance criterion (14).

The composite equation (4) reflects the contribution of various position and angular rates to the overall motion of the rover. In order to control the rover motion while maintaining the rover balance, we must determine commands to the wheels, steering and joints actuators. For this, we rearrange (4) into an equation of the form

$$A \dot{\chi} = B \dot{q} \quad (15)$$

where $\dot{\chi}$ is the $n_x \times 1$ vector of unknown quantities to be determined, and \dot{q} is the $n_q \times 1$ vector of known quantities. The unknown vector consists of actuation signals such as active suspension joints, wheel roll rates, and un-measurable quantities such as wheel-terrain contact angles and appropriate slips. The known vector consists of desired quantities such as the desired forward rover velocity \dot{x}_d and heading $\dot{\gamma}_d$ as well as sensed quantities such as pitch and roll rates $\dot{\alpha}$ and $\dot{\beta}$, and rocker angle rate $\dot{\rho}$. The matrices A and B are obtained from the elements of J and the identity matrices I_1, I_2, \dots, I_6 in (4). After partitioning (4) into the form (15), the dimensions of A and B are $6n \times n_x$ and $6n \times n_q$. In order to be able to solve (15) while minimizing (14), we must have an underdetermined system of equations, so that the null space of A can be used for optimization. In this case we can solve (15) subject to minimization of (12) as (Nakamura 1991)

$$\dot{\chi} = A^\# B \dot{q} - k(E - A^\# A) \begin{pmatrix} \partial f / \partial \sigma \\ 0 \end{pmatrix} \quad (16)$$

where $A^\#$ is the pseudo-inverse of A , k is a scalar, E is $n_x \times n_x$ identity matrix, $\partial F / \partial \sigma$ is the $n_\sigma \times 1$ vector of the gradient of the performance function with respect to the active suspension joints, and the zero vector had dimension $(n_x - n_\sigma) \times 1$. In the next section we specify the above quantities for our ARAS. The gradient can be computed numerically or analytically from (14).

4. SIMULATION RESULTS

In this section we present the results of balance control for the ARAS introduced in Section 2.1. The full Jacobian equation is not given here due to space limitations but is provided in (Mireles et al 2005). For the ARAS, the vector $\dot{\chi}$ in (15) is

$$\dot{\chi} = [\dot{\sigma} \quad \dot{y}_r \quad \dot{z}_r \quad \dot{\alpha}_r \quad \dot{\beta}_r \quad \dot{\delta} \quad \dot{u}_c \quad \dot{\phi}_c]^T \quad (17)$$

where $\sigma = [\sigma_1 \ \sigma_2]^T$ is the actuated hip vector; y_r, z_r and α_r, β_r are the unknown rover position and attitude angles; $\delta = [\delta_1 \ \dots \ \delta_4]^T$ is the contact angle vector, $u_c = [u_{c1} \ \dots \ u_{c4}]^T$ is vector of wheel contact translations, and $\phi_c = [\phi_{c1} \ \dots \ \phi_{c4}]^T$ is the vector of wheel contact rotations. Thus $\dot{\chi}$ is a 34×1 vector, and A is a $6n \times 34 = 24 \times 34$ matrix. Note that in general some rows of A are linearly dependent and thus $\text{rank}(A) \leq 24$. The vector of the known quantities in (15) is

$$\dot{q} = [\dot{x}_r \ \dot{\gamma}_r \ \dot{\rho} \ \dot{\psi}]^T \quad (18)$$

where \dot{x}_r and $\dot{\gamma}_r$ are the desired (specified) rover forward velocity and heading (yaw) rate, respectively, $\dot{\rho}$ is the measured rocker rate, and $\dot{\psi} = [\dot{\psi}_1 \ \dot{\psi}_2 \ \dot{\psi}_3 \ \dot{\psi}_4]^T$ is the steering angle rates vector. Note that since the axes of steering and wheel turn slip are coincident in this rover, the steering angles are indistinguishable from turn slip. In this case, a geometric approach is used to determine the steering angle rates $\dot{\psi}$ using the desired forward velocity \dot{x}_r and $\dot{\gamma}_r$ (Tarokh and McDermott 2005), and thus $\dot{\psi}$ is a known quantity. Thus the dimension of the known vector q is 7×1 , and B has the dimension 24×7 .

We have developed a simulation environment using Matlab/Simulink. We study the behavior of the rover for three terrains. Since the purpose of this study is balance control, in all cases we consider straight line motion to avoid mixing of different behaviors. The rover speed is set at 1 cm/s to ease the conversion between distance and time on the graphs.

Case 1: Inclined Terrain

The terrain and the trace of the rover wheels are shown in Fig. 6. The terrain is flat but has a 45 degrees slope which could result in tipover without actuated suspension. The hip angles start at their nominal values, e.g. $2\sigma_1 = 2\sigma_2 = 90$ degrees. The hip joint angles as given in Fig. 7 shows that the right joint has increased to raise the right side but the right angle is increased to lower the left side. This has almost leveled the rover as is evident by the rover roll angle shown in Fig. 8 where the initial roll angle of about 38 degrees has been reduced to about 13 degrees.

Case 2: Wavy and Bumpy Terrain

The terrain shown in Fig. 9 consists of a bump which is wavy (sinusoidal) under the left wheels and smooth under the right wheels. The hip joint angles are depicted in Fig. 10. It is interesting to note that the right and left hip joint values also go through sinusoidal type changes but in the opposite directions to maintain a level and balanced rover body. The rocker also shows sinusoidal behavior. The rover roll and pitch angles are seen in Fig. 11. The rover roll exhibits small changes due to the hip adjustments, whereas the rover pitch goes through relatively large variations due to the traversing up and then down the wavy bump.

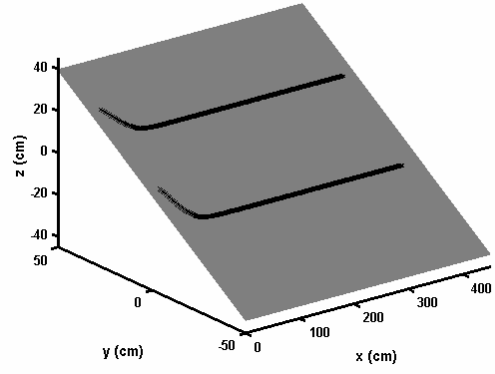


Fig. 6 Inclined terrain and traces of rover wheels

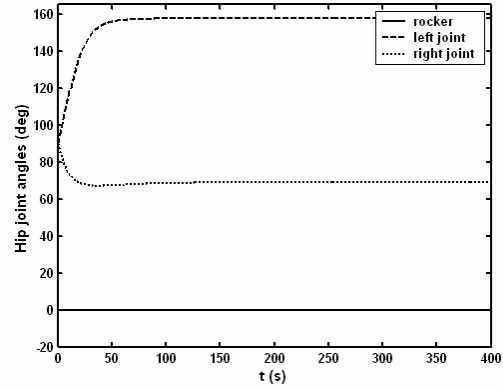


Fig. 7 Hip joint angle trajectories

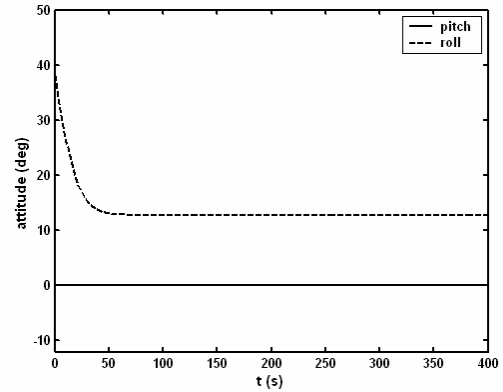


Fig. 8 Rover body roll and pitch angle profiles

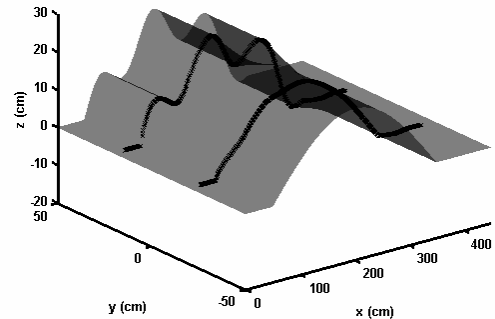


Fig. 9 Wavy and bumpy terrain

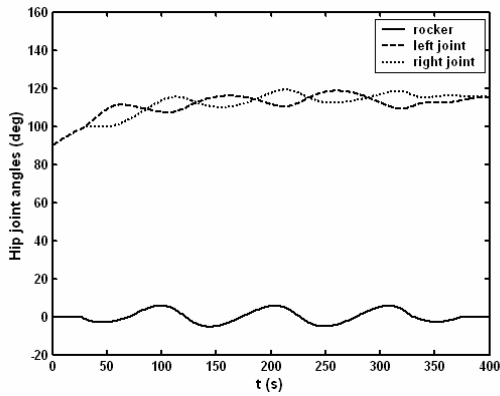


Fig. 10 Hip joint angle trajectories

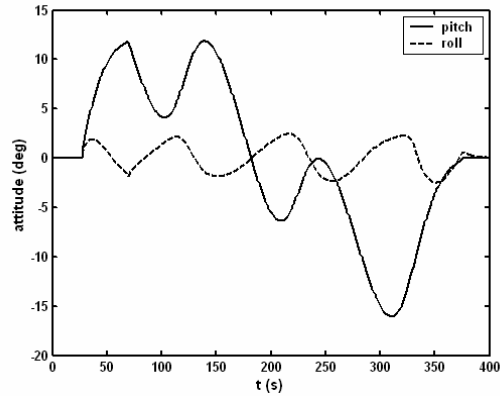


Fig. 11 Rover roll and pitch trajectories

Case 3: Inclined Ditch and Bump Terrain

In this case, the terrain has a slope of 45 degrees with a bump under the left side wheels and a ditch under the right side wheels as shown in Fig. 12. The hip angles are adjusted accordingly to balance the rover as shown in Fig. 13. The rover exhibits a maximum roll angle of about 16 degrees as seen from Fig. 14; much smaller than the 45 degree terrain slope.

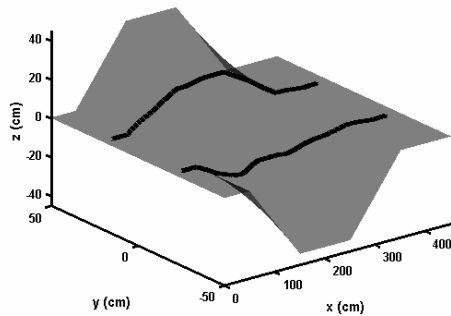


Fig. 12 Inclined ditch and bump terrain

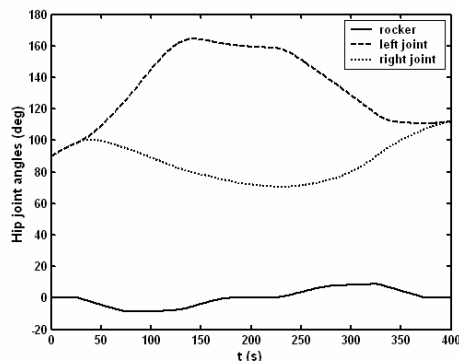


Fig. 13 Hip joint angle trajectories

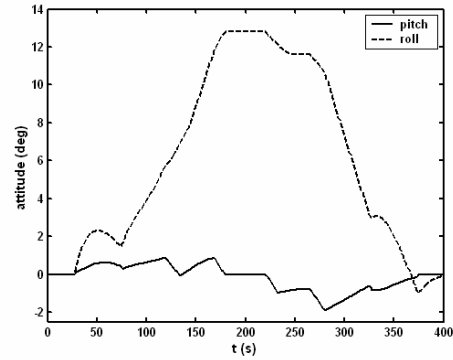


Fig. 14 Rover roll and pitch trajectories

5. CONCLUSIONS

A new methodology is presented for the kinematics modeling and control of articulated rovers for achieving rover balance when traversing rough and sloppy terrain. The main feature of the work is the formulation of rover kinematics which uses simple velocity propagation starting from wheel-terrain contact and going through various joints and linkages to finally reach the rover reference frame. This formulation makes the computer implementation very efficient through simple repeated function calls. Rover balance control is achieved through a pseudo-inverse method which optimizes balance criterion. The latter depends on the rover roll as well as angles between the rover gravity and certain vectors drawn from the rover reference to the wheel contact points. Application to the kinematics model of an articulated rover demonstrates that the proposed method is effective in achieving balance control.

REFERENCES

- Baerveldt, A.-J. Ed. (2002), *Agricultural Robotics, Autonomous Robots, Vol 13-1*, Kluwer Academic Publishers.
- Craig, J. Introduction to Robotics, Mechanics and Control (2005), pp.144-146, Pearson Prentice-Hall.
- Cunningham, J., J. Roberts, P. Corke and H. Durrant-Whyte (1998). Automation of underground LHD and truck haulage. *Proc. Australian IMM Conf.*, pp. 241-246.
- DeBolt, Ch., Ch. O'Donnell, S. Freed, and T. Nguyen, The bugs 'basic uxo gathering system' project for uxo clearance and mine countermeasures. *Proc. IEEE Int. Conf. Robotics and Automation*, pp. 329-334, Albuquerque, N.M., 1997.
- Gonthier, Y., and E. Papadopoulos (1998). On the development of a real-time simulator for an electro-hydraulic forestry machine. *Proc. IEEE Int. Conf. Robotics & Automation*, Leuven, Belgium.
- Iagnemma, K. and S. Dubowski (2003). Traction Control of wheel mobile robots in rough terrain with applications to planetary rovers. *Int. J. Robotics Res.*, vol. 23, No. 10-11, pp. 1029-1040.
- Mireles, L., G. McDermott and M. Tarokh (2005). Two approaches to kinematics modelling of articulated rovers. <http://www-rohan.sdsu.edu/~tarokh/lab/publications.html>
- Nakamura, N. (1991). *Advanced Robotics- Redundancy and Optimization*, Chapt. 4, Addison and Wesley.
- Schenker, P., T. Huntsberger, P. Pirjanian, E. Baumgartner, and E. Tunstel (2003). Planetary rover developments supporting Mars exploration, sample return and future human robotic colonization, *Autonomous Robots*, vol. 14, pp. 103-126.
- Sreenivasan, S. and K. Waldron (1996). Displacement analysis of an actively articulated vehicle configuration with extensions to motion planning on uneven terrain. *Trans. ASME J. Mechanical Design*, vol. 118, pp. 312-317.
- Tarokh, T. and G. McDermott. (2005) Kinematics Modeling and Analysis of Articulated Rovers. *IEEE Trans. Robotics*, vol. 21, No. 4, 539-553.
- Volpe, R. (2003). Rover functional autonomy development for Mars mobile science *Proc. IEEE Aerospace Conf.* pp. 643-652.